IOSR Journal of Applied Physics (IOSR-JAP)
e-ISSN: 2278-4861.Volume 18, Issue 5 Ser. 1 (Sep. – Oct. 2026), PP 36-48
www.iosrjournals.org

A Study of The Influence of Solar Wind Speed Disturbances on The Variations of Cosmic Rays

Anochili Lydia Uchenna[1], Chima Abraham Iheanyichukwu [2] and Otukaoha Collins Uche [3]
[123]Department of Industrial Physics, Enugu State University of Science and Technology, Agbani

ABSTRACT
A comprehensive study has been conducted to investigate the influence of solar wind disturbances on the periodic variations of cosmic rays. This research utilized data from three cosmic ray stations: APTY, ESOI, and OULU, covering a four-year period from 2011 to 2014. Additionally, solar wind speed data was incorporated into the analysis, which was performed using R statistical software. The study successfully identified a significant phenomenon known as Forbush decrease (FD), characterized by marked reductions in cosmic ray intensity. By employing a semi-automated method of FD selection, a considerable number of FDs were recorded and systematically analyzed. The findings revealed that the magnitude of FDs is influenced by the latitude and longitude of the respective cosmic ray stations. Moreover, a simultaneity test was conducted on the detected FDs, which demonstrated an overlap in the profiles of simultaneous events, emphasizing their strong magnitudes. The research also established a correlation between FD magnitudes and solar wind speed, highlighting the important role that solar wind disturbances play in triggering FDs. This insight contributes to our understanding of cosmic ray variations and their relationship with solar activity.
Keyword: *Cosmic rays,Forbush decrease,solar wind*

Date of Submission: 08-09-2026 Date of Acceptance: 17-09-2026

I. INTRODUCTION

Solar wind (SW) is a stream of charged particles emitted from the extremely hot corona of the Sun (Parker, 1958). These particles burst into interplanetary space, carrying with them a frozen solar magnetic field known as the Interplanetary Magnetic Field (IMF) (Dessler, 1967; Schatten, 2001). This solar release can occur through various phenomena, including solar flares, coronal mass ejections, and Corotating Interaction Regions (CIR) (Poudel *et al.,* 2019). In space, these charged particles interact with the Earth's magnetosphere through electromagnetic and viscous interactions, transferring energy and momentum within the system (Poudel *et al.,* 2019). The energy injected into the coupled magnetosphere-ionosphere environment causes distortions in geomagnetic activity, leading to various phenomena such as geomagnetic storms, substorms, and auroras (Gonzalez *et al.,* 1994). These distortions are collectively referred to as solar wind disturbances (Poudel *et al.,* 2019).

Furthermore, cosmic rays are high-energy particles that reach Earth from outer space (Ihongo and Wang, 2016). The majority of these cosmic rays originate from various regions within galaxies beyond our solar system and are collectively known as Galactic cosmic rays (GCRs). In contrast, a subset of cosmic rays, which are generated by the Sun, are referred to as solar cosmic rays (Ihongo and Wang, 2016). Notably, the intensity and flux of GCRs are significantly higher than those of solar cosmic rays (Abdullah and Jahan, 2017). Additionally, cosmic rays can also be produced by supernova explosions of dying stars, contributing to their vast sources (Abdullah and Jahan, 2017). These rays serve as messengers from the universe, providing crucial information about the fundamental building blocks of the cosmos and much more (Abdullah and Jahan, 2017).

The strength of cosmic rays and the speed of the solar wind (SWS) are both linked to fluctuations in solar activity, which exhibit variations over time (Kane, 2010). Cosmic ray Intensity (CRI) is influenced by a variety of factors, including the characteristics of the solar wind and the number of sunspots (Jacob *et al.,* 2020). Generally, it is understood that daily variations in cosmic ray intensity are related to changes in the primary radiation that interacts with the Earth's atmosphere (Brunberg and Dattner, 1954). Disturbances in the interplanetary medium caused by solar activity can lead to sudden, sharp decreases in the observed galactic cosmic ray (GCR) flux, known as Forbush Decreases (FDs) (Benjamin *et al.,* 2011).

A Forbush decrease represents an abrupt reduction in cosmic ray intensity, often accompanied by disturbances in the solar wind (Forbush, 1938; Lockwood, 1971). Since Forbush's discovery of FDs in 1937, significant effort has focused on identifying their solar sources, interplanetary structures, and underlying physical mechanisms (Lingri *et al.,* 2016). Initially, FDs were thought to be linked to solar flares, a view that persisted until the space age began (Lockwood, 1971). However, with the advent of space coronagraphs in the 1970s and subsequent observations of Coronal Mass Ejections (CMEs) and their Interplanetary Counterparts (ICMEs), it became evident that CMEs, rather than solar flares, are often the primary cause of Forbush Decreases (Lingri *et al.,* 2016). It is essential to note that not all observed ICMEs lead to Forbush decreases in GCR intensity (Lingri *et al.,* 2016). Further analysis of FDs reveals that the maximum decrease can exceed cosmic ray intensity by as much as 25% (Cane, 2000; Belov, 2008). Consequently, FDs are associated with strong solar phenomena such as CMEs (Lingri *et al.,* 2016). The most significant FDs are typically related to CMEs accompanied by shock waves (Cane, 2000; Lockwood, 1971; Mavromichalaki *et al.,* 2005; Papailiou *et al.,* 2012a).

FDs are observed and recorded at Earth by neutron monitors (NMs) (Lingri *et al.,* 2016). With their varying cut-off rigidities, these NMs are specifically designed to enhance the precision of FDs detection. Studies indicate that the magnitude of FDs is influenced by several factors, including the cut-off rigidity, latitude, longitude, and altitude of each monitoring station (Lingri *et al.,* 2016). This variability underscores the challenges that cosmic-ray particles encounter when attempting to penetrate the Earth's magnetic field (Lingri *et al.,* 2016). The valuable data obtained from NMs has been leveraged by researchers to better understand atmospheric disturbances. For example, McCracken *et al.* (2008) analyzed the ground level enhancement (GLE) event from 22 October 1989 using data from three NMs: THUL, SOPO, and MCMD. Additionally, Lingri *et al*. (2016) highlighted that FDs are typically more intense at the geomagnetic poles, opening avenues for further exploration of the relationship between cosmic events and Earth's atmospheric conditions. The detection of FDs is closely linked to the geomagnetic latitude and the Earth's position at any given moment (Lingri *et al.,* 2016).

Research by Okike and Umahi (2019) highlighted that significant increases in the magnitude of the FD were observed at the cosmic ray stations MCMD and SOPO, while the intensity variation recorded at another station, THUL, was relatively minor. Given that these three stations are situated at widely separated longitudes, as noted by McCracken *et al.,* (2008), the differences in FD characteristics can largely be attributed to their latitudinal positions and the proximity of THUL to the two other stations (Okike and Umahi, 2019). This observation strongly indicates that FDs are coordinate-dependent, reinforcing the idea that the characteristics of FDs can vary significantly across different cosmic ray stations.

Therefore, this work will study the characteristics of FDs selected from different cosmic-ray stations using a semi-automated approach.

2.1 Materials

This research was utilize the data daily CR intensity counts that was sourced from http://cr0.izmiran.ru/common/ for OULU, APTY, and ESOI CR stations. These CR stations have cutoff rigidities of 0.77 GV, 5.6 GV, and 10.8 GV, respectively. Their geographic coordinates are as follows: OULU at 65.06°N, 25.47°E; APTY at 67.55°N, 33.33°E; and ESOI at 33.3ºN 35.8ºE. The altitudes for these stations are 81 m, 117 m, and 1240 m, respectively. In addition, solar wind speed (SWS) data sourced from https://omniweb.gsfc.nasa.gov/ html/owdata.html , was incorporated into the analysis for the same timeframe, covering five years from 2011 to 2014. The statistical analysis was carried out using R statistical software on a laptop computer, ensuring a comprehensive evaluation of the data collected.

2.2 Methods

The daily cosmic ray data was sourced, organized, and structured within a text editor spreadsheet. All entries of timing (00 hours) in the CR data was filtered out to ensure the data focus solely on daily counts. Subsequently, the dataset consist of dates and their corresponding CR counts presented in a clear tabular format. Each CR station's data was saved with a unique filename for easy identification. Similarly, solar wind speed (SWS) data was sourced and structured in a comparable tabular format, covering the same timeframe as the CR counts. During the download process, the data was filtered by dates and counts using website data queries, and each set was also be saved with unique filenames.

For the selection of FDs, this research employed a semi-automated method utilizing a computer software program compatible with R statistical software. The FD event location program developed by Okike and Umahi (2019b) was implemented. The method involves several key processes:

(a) The program restructure the raw CR data into a unique format comprising dates and counts and save it with a distinct filename.

(b) It read the saved file from step (a), scale, and plot the daily variations of the CR counts for the period under study.

(c) The program normalized the daily CR counts, ensuring consistency and accuracy in the analysis using the following equation:

$$CR(\%) = \frac{CR - CRq}{CRq} \times 100\% \qquad (1.1)$$

(d) Additionally, the program plotted the normalized CR counts against their corresponding dates, illustrating decreases in CR count variations. This visualization established a baseline for FD detection by incorporating an ab-line to highlight variations in CR counts.
(e) A threshold of < -0.5% served as the baseline for selecting FD magnitudes, ensuring that only significant variations are considered.
(f) The program first filtered the observed variations, marking them with red plotted points for clarity. Subsequently, it filtered these variations a second time by inputting the identified FD dates and magnitudes, resulting in a refined depiction of FDs in the third plot. A list of FD dates and their corresponding magnitudes was compiled. Alongside this, the relevant solar wind speed (SWS) data was positioned beside the FDs, presented in a clear tabular format. Finally, correlation and regression analyses were conducted between selected FD magnitudes and the SWS, allowing for a thorough examination of the relationships between these variables.

II. RESULT

3.1Selection of Forbush Decreases

The graphical processes essential for FD selection are effectively illustrated in Figs 1, 2 and 3. Fig 5 presents the raw CR data, while Figs 6 and 7 showcase the first and second stages of filtration applied to the CR count, aimed at identifying FDs. In Table 1 below, the selected FD dates from three stations: APTY, ESOI, and OULU was provided. This table highlights a sample of FD dates for these three CR stations, with the full dataset available in Appendix I. The first column of features the serial number, followed by the event date for the APTY CR station in the second column. The third and fourth columns respectively list the FD dates for the APTY and ESOI CR stations, facilitating a clear comparison of the data.

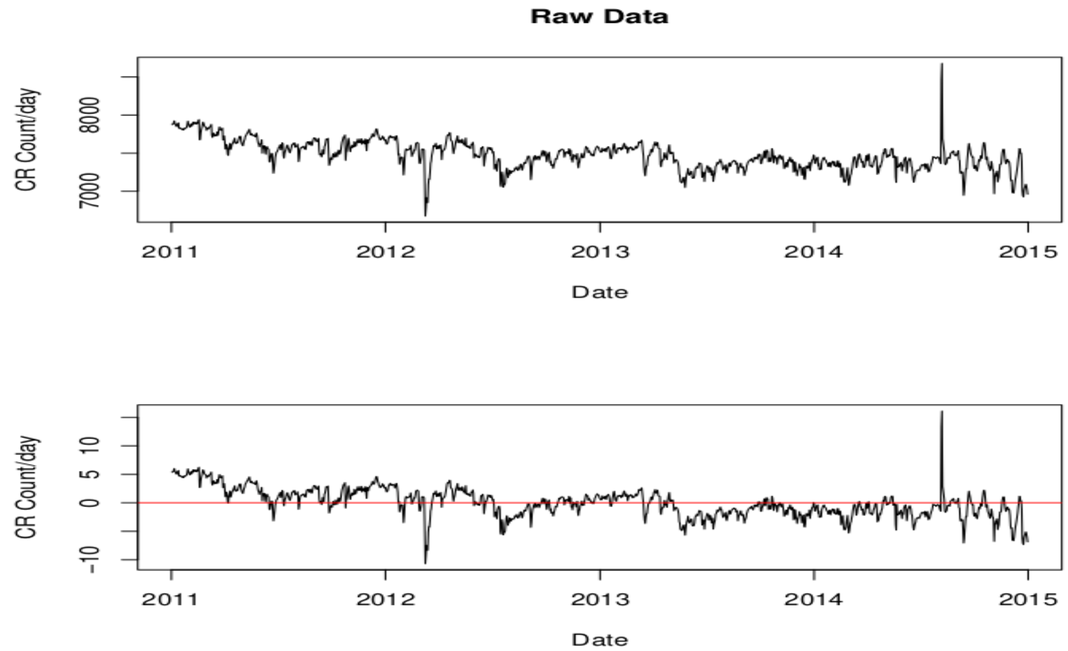

Year

(a)

Fig 1: Variations of raw CR counts

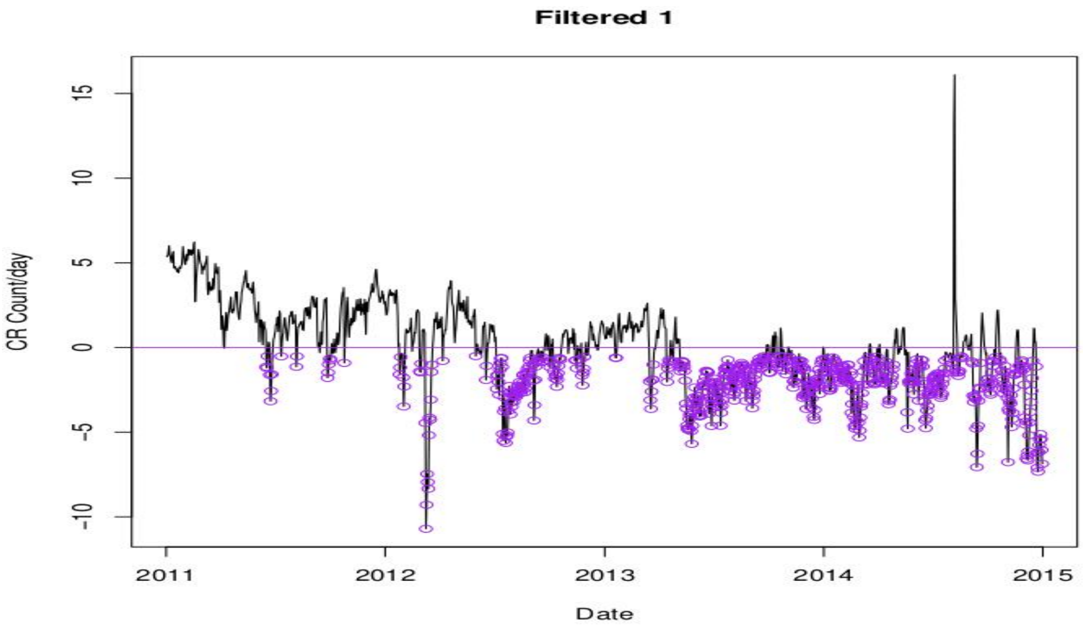

Year

Fig 2: First filtration of CR counts to detect FDs

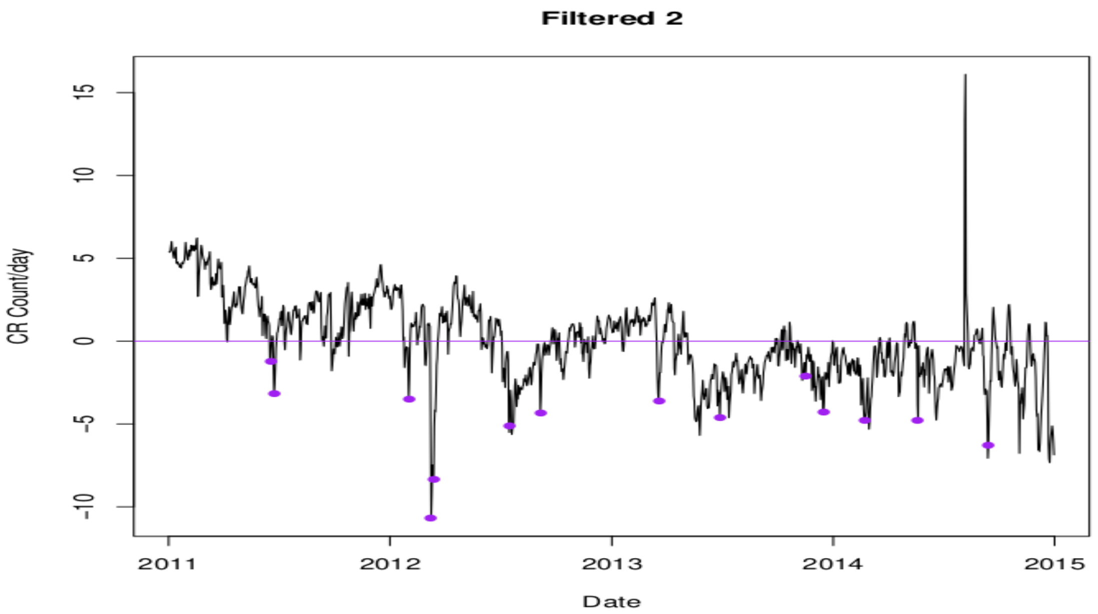

Year

Fig 3: Second filtration of CR counts to detect FDs

Table 1: Selected FD Dates

S/N	APTY DATE	ESOI DATE	OULU DATE
1	2011-04-07	2011-01-17	2011-04-08
2	2011-04-08	2011-01-31	2011-06-17
3	2011-06-11	2011-02-01	2011-06-18
4	2011-06-17	2011-02-02	2011-06-19
5	2011-06-18	2011-02-03	2011-06-20
6	2011-06-19	2011-02-04	2011-06-23
7	2011-06-20	2011-02-18	2011-06-24

8	2011-06-23	2011-02-20	2011-06-25
9	2011-06-24	2011-02-21	2011-06-26
10	2011-06-25	2011-02-26	2011-06-27
11	2011-06-26	2011-03-09	2011-06-28
12	2011-06-27	2011-03-10	2011-07-11
13	2011-06-28	2011-03-11	2011-07-12
14	2011-07-11	2011-03-12	2011-08-06
15	2011-07-12	2011-03-13	2011-08-07
16	2011-08-06	2011-03-14	2011-09-14
17	2011-08-07	2011-03-15	2011-09-27
19	2011-09-13	2011-03-17	2011-09-29
20	2011-09-14	2011-03-18	2011-09-30
21	2011-09-15	2011-03-19	2011-10-01
22	2011-09-18	2011-03-20	2011-10-02
23	2011-09-27	2011-03-22	2011-10-05
24	2011-09-28	2011-03-24	2011-10-06
25	2011-09-29	2011-03-25	2011-10-09
26	2011-09-30	2011-03-30	2011-10-10
27	2011-10-01	2011-04-05	2011-10-11
28	2011-10-02	2011-04-08	2011-10-15
29	2011-10-03	2011-04-09	2011-10-16
30	2011-10-05	2011-04-10	2011-10-25
31	2011-10-06	2011-04-11	2012-01-25
32	2011-10-07	2011-04-12	2012-01-26
33	2011-10-09	2011-06-17	2012-01-27
34	2011-10-10	2011-06-18	2012-01-31
35	2011-10-11	2011-06-23	2012-02-01
36	2011-10-15	2011-06-24	2012-02-02
37	2011-10-25	2011-06-25	2012-02-15
38	2012-01-23	2011-12-25	2012-02-16
39	2012-01-25	2011-12-26	2012-02-27

3.2. Forbush Decrease Magnitude

The FD magnitudes selected from the three CR stations—APTY, ESOI, and OULU—are systematically organized in Table 2 below. This table highlights the FD samples for each station alongside their corresponding SWS.

In Table 2, the first column presents the serial numbers, while the second column lists the event dates for the APTY CR station. The third and fourth columns provide vital data, detailing the FD magnitude and SWS for the APTY station. Continuing in the same structured manner, columns five, six, and seven capture the dates, magnitudes, and SWS for the ESOI CR station. Finally, columns eight, nine, and ten are dedicated to the distribution of FD dates, magnitudes, and SWS for the OULU CR station. This structured approach ensures clarity and ease of comparison across the different stations.

Table 2: List of FD Magnitudes with their corresponding SWS

	APTY			ESOI			OULU		
S/N	DATE	FD MAG (%)	SWS	DATE	FD MAG (%)	SWS	DATE	FD MAG (%)	SWS
1	2011-04-07	-0.57	514	2011-01-17	-1.06	490	2011-04-08	-0.51	430
2	2011-04-08	-0.73	430	2011-01-31	-2.13	277	2011-06-17	-1.56	470
3	2011-06-11	-0.53	403	2011-02-01	-2.54	414	2011-06-18	-1.73	415

4	2011-06-17	-1.82	470	2011-02-02	-2.68	441	2011-06-19	-1.18	396
5	2011-06-18	-1.88	415	2011-02-03	-1.87	344	2011-06-20	-0.54	395
6	2011-06-19	-1.19	396	2011-02-04	-0.82	399	2011-06-23	-2.17	605
7	2011-06-20	-0.62	395	2011-02-18	-0.68	526	2011-06-24	-3.57	610
8	2011-06-23	-2.3	605	2011-02-20	-1.04	428	2011-06-25	-3.03	583
9	2011-06-24	-3.84	610	2011-02-21	-0.66	394	2011-06-26	-2.03	528
10	2011-06-25	-3.24	583	2011-02-26	-0.53	316	2011-06-27	-1.03	445

	APTY			ESOI			OULU		
S/N	DATE	FD MAG (%)	SWS	DATE	FD MAG (%)	SWS	DATE	FD MAG (%)	SWS
11	2011-06-26	-2.26	528	2011-03-09	-2.95	319	2011-06-28	-0.6	386
12	2011-06-27	-1.11	445	2011-03-10	-5.7	333	2011-07-11	-0.59	520
13	2011-06-28	-0.65	386	2011-03-11	-5.72	406	2011-07-12	-0.97	681
14	2011-07-11	-0.75	520	2011-03-12	-4.8	528	2011-08-06	-1.73	535
15	2011-07-12	-1.21	681	2011-03-13	-4.15	555	2011-08-07	-1.27	539
16	2011-08-06	-1.82	535	2011-03-14	-3.6	561	2011-09-14	-0.57	518
17	2011-08-07	-1.21	539	2011-03-15	-2.66	474	2011-09-27	-2.33	604
19	2011-09-13	-0.57	579	2011-03-17	-1.2	398	2011-09-29	-1.57	539
20	2011-09-14	-0.99	518	2011-03-18	-1.06	368	2011-09-30	-1.14	454
21	2011-09-15	-0.57	458	2011-03-19	-0.74	346	2011-10-01	-1.1	495
22	2011-09-18	-0.5	441	2011-03-20	-0.54	351	2011-10-02	-1.16	488
23	2011-09-27	-2.47	604	2011-03-22	-0.55	351	2011-10-05	-0.57	420
24	2011-09-28	-2.15	486	2011-03-24	-1.11	461	2011-10-06	-0.86	376
25	2011-09-29	-1.67	539	2011-03-25	-0.91	435	2011-10-09	-0.86	333
26	2011-09-30	-1.15	454	2011-03-30	-0.68	361	2011-10-10	-1.1	343
27	2011-10-01	-1.34	495	2011-04-05	-0.55	485	2011-10-11	-0.62	364
28	2011-10-02	-1.44	488	2011-04-08	-1.15	430	2011-10-15	-0.86	444
29	2011-10-03	-0.83	399	2011-04-09	-0.5	429	2011-10-16	-0.59	451
30	2011-10-05	-0.89	420	2011-04-10	-0.51	365	2011-10-25	-1.57	484
31	2011-10-06	-1.03	376	2011-04-11	-0.51	366	2012-01-25	-1.68	574
32	2011-10-07	-0.77	375	2011-04-12	-1.3	535	2012-01-26	-1.19	468
33	2011-10-09	-0.7	333	2011-06-17	-0.74	323	2012-01-27	-0.57	509
34	2011-10-10	-0.99	343	2011-06-18	-0.67	359	2012-01-31	-1.78	363
35	2011-10-11	-0.7	364	2011-06-23	-0.69	390	2012-02-01	-3.33	380
36	2011-10-15	-0.53	444	2011-06-24	-1.3	426	2012-02-02	-2.16	408
37	2011-10-25	-1.59	484	2011-06-25	-0.69	482	2012-02-15	-0.89	381
38	2012-01-23	-0.69	428	2011-12-25	-4.64	359	2012-02-16	-0.52	374
39	2012-01-25	-2.27	574	2011-12-26	-4.33	326	2012-02-27	-0.59	468
40	2012-01-26	-1.86	468	2011-12-27	-2.86	259	2012-02-28	-1.97	426
41	2012-01-27	-1.25	509	2011-12-28	-2.36	273	2012-02-29	-1.79	448
42	2012-01-28	-1.02	463	2011-12-29	-2.22	358	2012-03-01	-1	456
43	2012-01-29	-1.09	413	2011-12-30	-2.02	382	2012-03-08	-5.32	602
44	2012-01-30	-1.06	380	2011-12-31	-1.96	361	2012-03-09	-11.3	668
45	2012-01-31	-2.44	363	2012-01-01	-2.23	368	2012-03-10	-8.82	520
46	2012-02-01	-4.14	380	2012-01-02	-4.33	362	2012-03-11	-7.25	436
47	2012-02-02	-2.97	408	2012-01-03	-3.63	392	2012-03-12	-7.78	524

48	2012-02-03	-1.1	412	2012-01-04	-3.59	348	2012-03-13	-8.54	621
49	2012-02-15	-0.91	381	2012-01-05	-3.49	322	2012-03-14	-5.68	520
50	2012-02-16	-0.54	374	2012-01-06	-3.95	419	2012-03-15	-5	609

3..3.Forbush Decrease Simultaneity

The variations illustrated in Fig 8 demonstrate the simultaneity of February 1, 2012 FD event. A sample of these simultaneous FDs is presented in Table 3 while the comprehensive list of simultaneous FDs in this research is presented in Appendix II. In Fig. 8, an overlap of the FD onset counts, the minimum decrease, and the recovery phase for the selected FDs was observed. This visualization effectively highlights the relationships and dynamics among the events during the specified period.

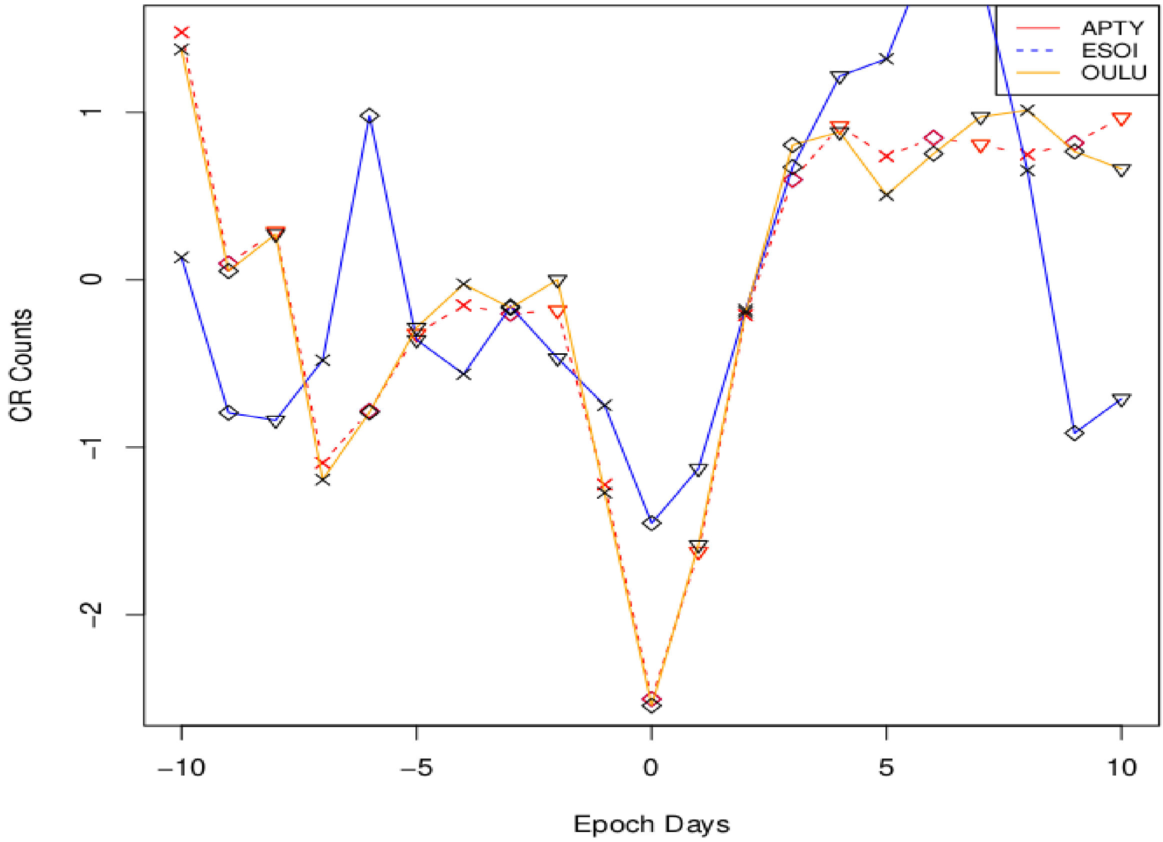

Fig .4: FD Simultaneity

Table 3: Sample of Simultaneous Forbush Decreases

S/N	DATE	APTY	ESOI	OULU
1	2011-04-08	-0.73	-1.15	-0.51
2	2011-06-17	-1.82	-0.74	-1.56
3	2011-06-18	-1.88	-0.67	-1.73
4	2011-06-23	-2.3	-0.69	-2.17
5	2011-06-24	-3.84	-1.3	-3.57
6	2011-06-25	-3.24	-4.64	-3.03
7	2012-01-25	-2.27	-10.94	-1.68
8	2012-01-26	-1.86	-8.78	-1.19
9	2012-01-27	-1.25	-10.76	-0.57
10	2012-01-31	-2.44	-11.33	-1.78
11	2012-02-01	-4.14	-12.38	-3.33
12	2012-02-02	-2.97	-11.89	-2.16
13	2012-02-15	-0.91	-9.63	-0.89

14	2012-02-16	-0.54	-10.59	-0.52
15	2012-02-27	-0.77	-9.48	-0.59
16	2012-02-28	-2.08	-10.44	-1.97
17	2012-02-29	-2.15	-11.65	-1.79
18	2012-03-01	-1.63	-12.82	-1
19	2012-03-08	-5.11	-12.79	-5.32
20	2012-03-09	-11.32	-13.89	-11.31
21	2012-03-10	-9.91	-12.08	-8.82
22	2012-03-11	-8.1	-10.66	-7.25
23	2012-03-12	-8.58	-8.98	-7.78
24	2012-03-13	-8.97	-8.49	-8.54
25	2012-03-14	-5.83	-7.55	-5.68
26	2012-03-15	-4.81	-9.64	-5
27	2012-03-16	-4.93	-10.96	-4.76
28	2012-03-17	-3.74	-9.58	-3.44
29	2012-03-18	-2.12	-8.76	-2.17
30	2012-03-19	-1.7	-7.59	-1.89
31	2012-03-20	-0.7	-6.27	-1.08
32	2012-07-20	-6.28	-1.28	-0.84
33	2012-07-21	-5.91	-1.3	-5.51
34	2012-07-22	-5.84	-1.27	-5.47
35	2012-07-23	-5.67	-1.35	-5.54
36	2012-07-24	-4.41	-0.95	-4.29
37	2012-07-26	-2.95	-0.55	-2.87
38	2012-07-27	-3.31	-0.75	-3.25
39	2012-07-28	-4.61	-0.71	-4.41
40	2012-12-04	-1.13	-0.65	-1.21

3.4.Correlation between Forbush Decrease Magnitude and Solar Wind Speed

The results of the correlation analysis between the FD magnitudes of the three stations and their corresponding solar wind data are presented in Table The Pearson r correlation method was employed for this analysis. Table 4 displays the correlation values for the FD magnitudes from the APTY, ESOI, and OULU CR stations in relation to their solar wind speeds. Additionally, Figs. 5, 6, and 7 illustrate the correlation plots between the FDs and SWS.

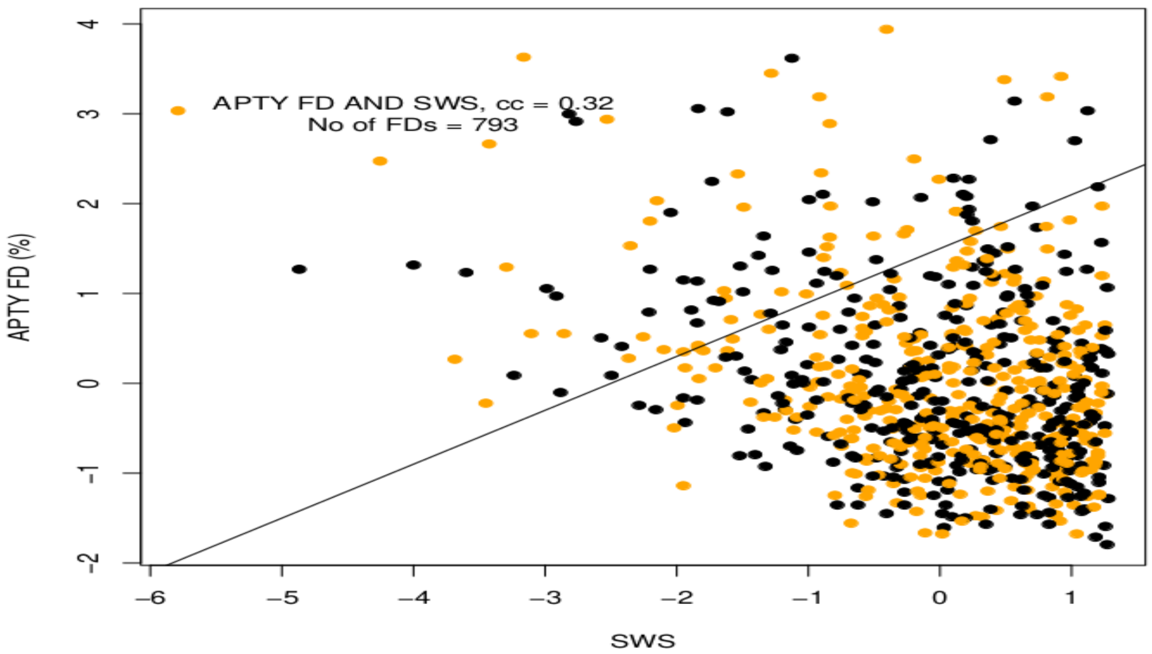

Fig.5: Correlation of APTY FD and SWS

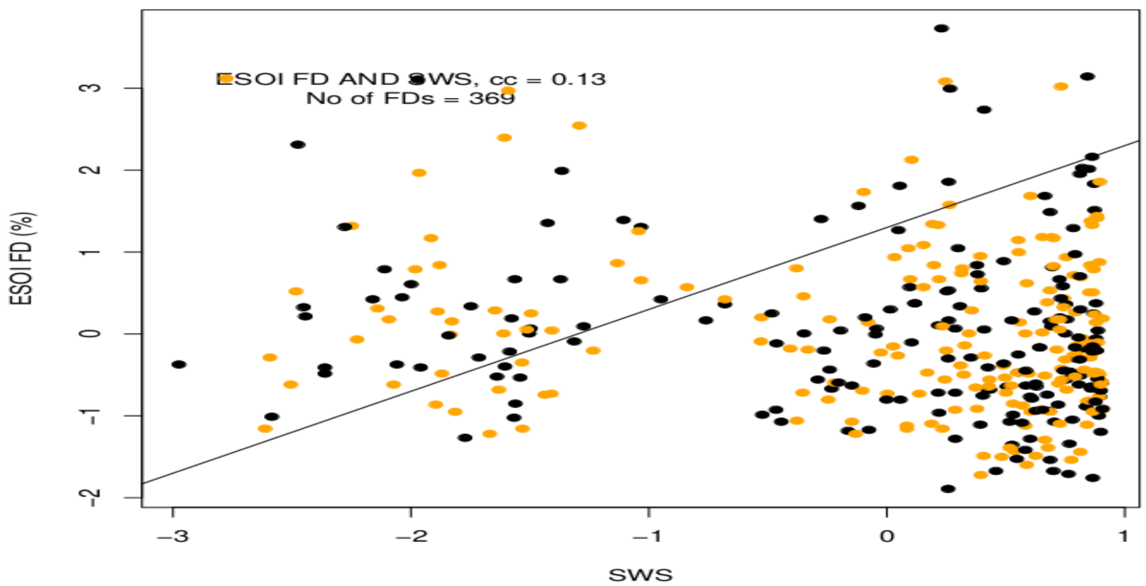

Fig.6: Correlation of ESOI FD and SWS

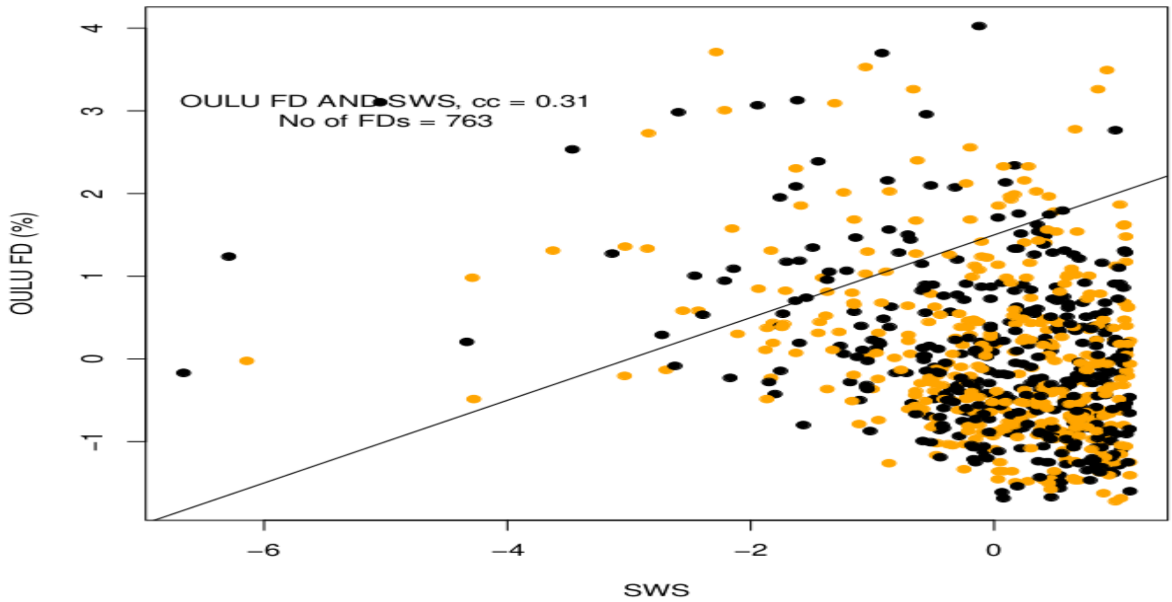

Fig. 7: Correlation of OULU FD and SWS

IV.DISCUSSION

4.1 Selection of Forbush Decrease

Recent studies on Forbush Decreases (FDs) have highlighted various methodologies for their selection: (i) manual, (ii) semi-automated, and (iii) automated methods. These approaches have been effectively utilized by a range of researchers in identifying FDs. For instance, Okike *et al.* (2021) successfully detected 513 and 503 FDs for the OULU and INVK Cosmic Ray (CR) stations, respectively, during solar cycle 23, utilizing the automated selection method. Similarly, Kristjansson *et al.* (2008) identified 22 significant FDs for Climax CR counts from 2000 to 2005 using the manual method. Their validation process involved cross-referencing FD dates with data from the Oulu and Moscow stations.

In this study, raw CR counts from APTY, ESOI, and OULU CR stations were analyzed using a semi-automated method to identify and select FDs. The results were notable: APTY recorded a remarkable 793 FDs, while ESOI and OULU reported 369 and 763 FDs, respectively. A comparative analysis revealed both similarities and variations in FD dates across these stations, with instances of simultaneous FDs and non-simultaneous events.

The result of this study indicated that APTY had the highest number of FDs, which may be linked to its geographic coordinates: 67.55°N, 33.33°E. OULU, with its coordinates of 65.06°N, 25.47°E, followed closely behind, while ESOI, positioned at 33.3°N, 35.8°E, reported the fewest FDs. This trend supports the findings of Tezari and Mavromichalaki (2016), which suggest that the occurrence of FDs is influenced by both longitudinal and latitudinal factors.

Generally, the findings of this study reinforce existing research regarding the coordinate dependency of FDs, offering valuable insights into the geographical aspects that may affect their frequency and occurrence.

4.2 Forbush Decrease Magnitude

The magnitude of a Forbush Decrease (FD) refers to the degree of decrease in cosmic ray intensity. Tables present the determined FD magnitudes for the CR stations APTY, ESOI, and OULU. Previous research indicates that the magnitude of FDs is influenced by the latitudes of neutron monitors. For example, Tezari and Mavromichalaki (2016) suggested that FDs depend on both longitudinal and latitudinal factors. The results of this study revealed a consistent pattern in the recorded magnitude of FDs, which decreased from the lower latitude neutron monitor at ESOI to the higher latitude station at APTY. Specifically, for the event on January 2, 2012, the magnitudes recorded were -12.38%, -4.14%, and -3.33% for the ESOI, OULU, and APTY stations, respectively. Moreover, the events of June 24, 2011, occurred in close temporal proximity and displayed similar patterns across the three stations, as illustrated in Fig. 9. While ESOI registered the most pronounced depression, followed by OULU, APTY exhibited the least significant drop in intensity.

These findings suggest a strong correlation between FD magnitude and the geographic coordinates of the cosmic ray detectors. Notably, strong Forbush Decreases tend to exhibit a clear and substantial drop in intensity, whereas weaker events do not show as pronounced a depression. These weaker FDs are often categorized as non-simultaneous events (Oh, Yi, and Kim, 2008; Okike and Collier, 2011a) that may not be detected by all stations.

Tezari et al. (2016) indicated that these weaker events are influenced by diurnal anisotropy, which affects their visibility.
For the purpose of FD selection in this study, a baseline magnitude of -0.5% was established. Consequently, cosmic ray depressions that exceeded this threshold were not classified as FDs in this analysis. This criterion helps to ensure that only significant FDs are considered in the findings, underlining the importance of magnitude in understanding these phenomena.

4.4 FD Simultaneity

Simultaneous FDs are defined as those Forbush Decreases that occur globally at the same time or on the same day. The determination of FD simultaneity across different CR stations relies on the overlap of the FD's main phase, which encompasses the period during which cosmic ray intensity decreases before returning to a recovery phase. Researchers have employed various techniques to assess the simultaneity of FD events. For example, Pankaj and Shukla (1994) and Kane (2010) utilized time series analysis (SEA), based on the premise of global simultaneity of FDs at one or more stations. Their approaches often considered similarities or differences in key parameters such as onset time, maximum decrease, main phase, and recovery phase, both before and after the occurrence of FDs.

The precise timing of an FD event's global observation is critical in these studies, with epoch time typically identified as either the moment of maximum decrease in galactic cosmic ray (GCR) intensity or the onset of the FD itself. However, Kane (2010) expressed skepticism regarding conclusions drawn from such studies, suggesting that data from a single location might not adequately represent global cosmic ray effects. This highlights the importance of analyzing global simultaneity of FDs using comprehensive cosmic ray data from neutron monitors located across the entire Earth, rather than relying on a single station.

In this study, epoch analysis was employed as the method for the simultaneity test. The FD simultaneity dates for the APTY, ESOI, and OULU stations are presented in Table 3. Notably, the magnitudes of these simultaneous events were significantly higher compared to non-simultaneous events, reinforcing the idea that simultaneous FDs tend to be stronger, while non-simultaneous events are typically weaker. For instance, the event on February 1, 2012, exhibited high magnitudes across all three stations. Fig 7 illustrates the cosmic ray intensity profile for this simultaneous FD event recorded at the APTY, ESOI, and OULU NM stations during 2012. The main phases of the FD event at each station showed clear overlap in the cosmic ray intensity profile, regardless of their geographical locations, further validating that these events are indeed simultaneous.

Thus, the results of the simultaneity test conducted in this study align with previous research, supporting the notion of overlapping FDs observed across multiple neutrons monitor stations.

4.5 Correlation Test

Previous research has indicated that the magnitude of Forbush Decreases (FDs) observed at stations with similar latitudes tends to exhibit a strong positive correlation. Additionally, FDs have been shown to correlate with solar activities. Todd and Kniveton (2001) analyzed FDs at three high-latitude stations (NWRK, MCMC, and SOPO). While they did not report specific outcomes of their comparisons or address the implications of their results, a common underlying assumption in the field is that simultaneous FDs at two or more stations are indicative of strong events. Between 2000 and 2005, Kristjansson *et al.* (2008) identified 22 FDs using data from the CLMX station. They compared their FD event days with those recorded at Oulu and Moscow neutron monitors and assumed, without extensive justification, that their FDs were consistent or simultaneous with those from the other locations.

Similarly, previous studies have demonstrated a correlation between FD magnitude and solar activities. For instance, Belov *et al*. (2001) highlighted the correlation between FD magnitude and solar wind speed (SWS). In the current study, we aimed to analyze the correlations between FD magnitudes and solar wind speed to further explore their relationship. Table 3 presents the results of the correlation test between the FD magnitudes recorded at the three stations of APTY, ESOI, and OULU with solar wind speed. A stronger correlation was observed between FD magnitudes and solar wind across all three stations. For example, the correlation coefficients for the FD magnitudes of APTY and OULU CR stations with solar wind speed were cc = 0.32 and cc = 0.31, respectively, while the correlation for the ESOI CR station with solar wind speed was cc = 0.13. Similarly, the alignment of the plotted points in Figs 9, 10 and 11 indicates a good correlation between the FD magnitudes of the three CR stations and SWS.

These findings suggest that disturbances in solar wind are associated with the occurrence of FDs. Notably, the highest correlation was found between the FD magnitudes of APTY CR station and solar wind speed, reinforcing the idea that solar activities play a significant role in the generation of FDs. Generally, the strong correlations observed between solar wind speed and FD magnitudes provide compelling evidence of the influence of solar activity on these cosmic ray phenomena.

5.1 Summary

The summary of this study is organized according to the objectives, corresponding results, and discussions, as outlined below.

The semi-automated method of FD selection employed in this research successfully identified a notable number of FDs from the three cosmic ray (CR) stations of APTY, ESOI, and OULU. These findings contribute valuable data to the existing catalogue of FDs within cosmic ray research.

It was observed that FD magnitudes are influenced by the coordinates of the CR stations. Specifically, the magnitude of the FDs consistently increased from the lower latitude station at ESOI to the higher latitude station at APTY.

Furthermore, the magnitudes of simultaneous FD events were significantly higher compared to those of non-simultaneous events, reinforcing the assertion that simultaneous events are associated with stronger decreases in cosmic ray intensity, while non-simultaneous events are generally weaker. Additionally, the main phases of the simultaneous FD events recorded at each NM station displayed notable overlap in the cosmic ray intensity profiles, irrespective of the stations' locations.

Finally, a correlation was established between FD magnitudes and solar wind speed, suggesting that FDs are indeed influenced by disturbances in solar wind activity. These results underscore the relationship between solar phenomena and cosmic ray behavior, highlighting the impact of solar wind on the occurrence and intensity of FDs.

5.2 Conclusion

Solar wind disturbances play a crucial role in influencing cosmic ray intensity, resulting in notable variations. This process culminates in a significant decrease in cosmic ray intensity, referred to as a Forbush decrease, highlighting the interconnectedness of solar activity and cosmic ray behavior.

REFERENCES

[1]. Abdullah A.l. Zaman MD, Jahan Monira N. (2017). Variation of Cosmic Ray Intensity during
[2]. Different Types of Solar Eclipses from 1990 to 2017 (August). *J Space Explor*., *6*(3),135.
[3]. AMS collaboration (2000). Cosmic Proton. *Phys. Lett.* B490, 27
[4]. AMS collaboration (2000). Leptons in near earth orbit. *Phys. Lett*., B494, 193
[5]. Barbashina N, Ampilogov N, Astapov I, Borog V, Dmitrieva A, Kovylyaeva A, Kokoulin R,
[6]. Kompaniets K, Mannocchi G, Mishutina Y. Petrukhin A, Saavedra O, Shutenko V, Sit'ko O, Trinchero G, Yakovleva E, Yashin I (2009). Local anisotropy of muon flux during Forbush decreases from URAGAN data. *In: Proceedings of the 31st International Cosmic Ray Conference,* Łód´z, 1
[7]. Barnden, L.R. (1973). Forbush Decreases 1966–1972; Their Solar and Interplanetary
[8]. Associations and Their Anisotropies. *In: Proceedings of the 13th International Cosmic Ray Conference,* 2, 1277.
[9]. Belov A. V., Eroshenko E. A., Oleneva V. A., Struminsky, A. B. and Yanke V. G. (2001). What Determines the Magnitude of Forbush Decrease? *Adv. Space Rex.,* 27(3),625-630
[10]. Belov, A.V., Baisultanova, L., Eroshenko, E., Mavromichalaki, H., Yanke, V., Pschelkin, P., Plainaki, C., Mariatos, G. (2005). The new Athens center on data processing from the neutron monitor network in real timeJ. *Geophys. Res*., 110.
[11]. Benjamin Laken, Dominic Kniveton, and Arnold Wolfendale (2011). Forbush decreases, solar irradiance variations, and anomalous cloud changes. *Journal of Geophysical Research*, 116, D09201
[12]. Bird, D.J., *et al*. (1993). Evidence for correlated changes in the spectrum and composition of cosmic rays at extremely high energies. *Physical Review Letters,* 71, 3401 – 3404
[13]. Bird, D.J., *et al.* (1994). The cosmic ray energy spectrum observed by the Fly's Eye. *Astrophys. J.,* 424, 491 – 502
[14]. Brownlee R. G., *et al.* (1968). The arrival directions of high energy cosmic ray primaries. *Can. J. Phys.*, 46, S259
[15]. Burlaga, L., Sittler, E., Mariani, F. and Schwenn, R. (1981) Magnetic Loop behind an Interplanetary Shock: Voyager, Helios, and IMP 8 Observations. *Journal of Geophysical Research*: *Space Physics*, 86, 6673-6684.https:/ /doi.org /10.1029/ ja086ia08p06673
[16]. Cane, H.V., Richardson, I.G. and von Rosenvinge, T.T. (1996). Cosmic ray decreases: 1964 – 1994. *J. Geophys. Res.,* 101(A10), 21561.
[17]. Cane, H.V. (2000) Coronal mass ejections and Forbush decreases. *Space Sci. Rev. 93*,55.
[18]. Cocconi, G. (1956). Intergalactic Space and Cosmic Rays. *Nuovo Cimento, 10th ser*., 3, 1433 – 1442
[19]. Corbató, S. C., and Dai, H. Y. (1992). Design considerations for a super Fly's Eye experiment. *Nuclear Physics B-Proceedings Supplements,* 28(2), 176-180.
[20]. Cronin J. W. (1992). The Pierre Auger Observatory Design Report. *Nucl. Phys. B* (Proc. Suppl.) 28B, 213
[21]. Desiati l. Lazarian R. (2013). Anisotropy of TeV Cosmic Rays and outer Heliospheric
[22]. Boundaries. *The Astrophysical Journal*, *762*,44,10.
[23]. Fluckiger, E.O. (1991). A new Concept for the Simulation and Visualization of Cosmic Ray Particle Transport in the Earth's Magnetosphere. *In: Proceedings of the 22nd International Cosmic Ray Conference,* 5, 273
[24]. Forbush, S.E. (1958) Cosmic-Ray Intensity Variations during Two Solar Cycles. *Journal of Geophysical Research,* 63, 651-669. https://doi.org/10.1029/JZ063i004p00651
[25]. Ghosh, K., Raychaudhuri, P. (2006a). Time Variations of the Forbush Decrease Data. *J. Astrophys.* Astro-Ph/0701860, online link-http://adsabs.harvard.edu/cgi-bin/bib_query? arXiv:astro-ph/0701860
[26]. Greisen K. (1966). End to the Cosmic-Ray Spectrum? *Phys. Rev. Lett.*, 16, 748
[27]. Hayashida N., *et al*. (1994). Observation of a Very Energetic Cosmic Ray Well Beyond the Predicted 2.7 K Cutoff in the Primary Energy Spectrum. *Phys. Rev. Lett.,* 73, 3491
[28]. Hess V. F., (1912). Penetrating Radiation in Seven Free Ballon Flights. *Physics Zeits*, 13 (1084), 1-4.

[29]. Ifedili, S.O. (1996). Spacecraft measurement of Forbush decreases in the cosmic radiation. *Sol. Phys.*, 168, 195
[30]. Ifedili, S.O. (1997). Forbush Decreases in the Cosmic Radiation: Measurement of the Extent of the Modulating Region. Planet. *Space Sci.* 45, 511
[31]. Ifedili, S.O. (2004). The two-step Forbush decrease: An empirical model. *J. Geophys. Res.*, 109 (12), A02117
[32]. Ihongo, and Wang, (2016). The effects of solar wind on galactic cosmic ray flux at Earth. *Astrophysics and Space Science, 44*:1-9
[33]. Jeffery J. L., Joshua E. R. (2012). Sunspot Random Walk and 22-YearsVariations, *Geophysical Research Letters*, 39,10103, doi:10.1029/2012GL051818.
[34]. Kane, R.P. (2010). Severe geomagnetic storms and Forbush decreases: interplanetary relationships re- examined. *Ann. Geophys*. *28*, 479.
[35]. Lawrence, M. A., Reid, R. J. O., Watson A. A. (1991). The cosmic ray energy spectrum above 41017 eV as measured by the Haverah Park array. *J. Phys. G Nucl. Part. Phys.* 17, 733
[36]. Lee, S., Oh, S., Yi, Y., Evenson P., Jee G., and Choi H. (2015). Long-term Statistical Analysis of the Simultaneity of Forbush Decrease Events at Middle Latitudes. *J. Astron. Space Sci.,* 32(1), 33-38
[37]. Li, K. J., Zhang J., and Feng, W. (2017). Periodicity for 50 yr of daily solar wind velocity, *Monthly Notices of the Royal Astronomical Society*, 472(1),289–294.
[38]. Lockwood, J.A. (1971). Forbush Decreases in the Cosmic Radiation. *Space Sci. Rev*. 12, 688
[39]. Lockwood J. A., Webber W.R. and Debrunner H. (1991a). Forbush Decreases Interplanetary Magnetic field disturbances: Association with magnetic clouds, *JGR*, 96, 11587–11604. http://dx.doi.org/10.1029/91JA01012.
[40]. Mavromichalaki, H., Papaioannou, A., Petrides, A., Assimakopoulos, B., Sarlanis, C., Souvatzoglou Mertsch and Funk (2015). Solution to the cosmic ray anisotropy problem. *Phys. Rev. Lett.* 114.
[41]. Ngobein, M. D. (2006). Aspect of the modulation of cosmic Ray and sunspot in the outer Heliosphere. *Journal of space particles*, 35(17),182-204.
[42]. Nishida, A. (1983). Numerical Modeling of the Energy Spectrum of the Cosmic-Ray Forbush Decrease. *J. Geophys. Res.,* 88, 785
[43]. Oh, S.Y. Yi, Y. (2009). Statistical reality of globally nonsimultaneous Forbush decrease events. *J. Geophys. Res. 114*, A11102.
[44]. Oh, S.Y., Y Bidoli i, Y. and Kim, H.Y. (2008). Globally simultaneous Forbush decrease events and their implications. *J. Geophys. Res. 113*, A01103.
[45]. Okike, O. and Collier, A.B. (2011a). A multivariate study of Forbush decrease simultaneity. *J. Atmos. Solar-Terr. Phys.* 73, 796.
[46]. Okike and Umahi, D.E.(2019). The Empirical Implication of Conducting a Chree Analysis Using Data from Isolated Neutron Monitors. *Solar Phys, 294*,16.
[47]. Okike, O. (2020a). Automated detection of simultaneous/non-simultaneous Forbush decreases and the associated cosmic ray phenomena, *Journal of Atmospheric and Solar-Terrestrial Physics*, 211,1364-6826
[48]. Oloketuyi J., Liu Y., and Zhao M. (2019). The periodic and temporal behaviors of solar X-ray flares in solar cycles 23 and 24, *Re Astrophysical Journal*, 874(1),20.
[49]. Parker, E.N. (1963). Interplanetary Dynamical Processes. Wiley, New YorkPerkins, D. (2003). Particles Astrophysics. Reviewed Astrophysics, Oxford University Press, 289-331.
[50]. Poudel, P., Simkhada, S., Adhikari, B., Sharma, D., & Nakarmi, J. J. (2019). Variation of solar wind parameters along with the understanding of energy dynamics within the magnetospheric system during geomagnetic disturbances. *Earth and Space Science*, *6*,276–293.
[51]. Richardson I.G and Cane H.V (2002). Sources of Geomagnetic Activity during nearly three olar cycle (1972-2000), *Journal of Geophysical Research*, 107(8), 1187
[52]. Rolfs, C.E. and William, S.R. (1988). Cauldrons in the cosmos. The University of Chicago Press, ISBN 0-226-72456-5.
[53]. Schatten, K. H. (2001). Coronal and interplanetary magnetic field geometry: Streak lines.
[54]. Shah, G.N., *et al*.: (2005). Are Elementary Particle Masses Related? In: Proceedings of 29th International Cosmic Ray, 9, 219
[55]. Usoskin, I., Desorgher, L., Velinov, P. I. Y., Storini, M., Flueckiger, E., Buetikofer, R. and Kovalstov, G. A. (2009). Solar and galactic cosmic rays in the Earth's atmosphere, *Acta. Geophys.,* 57(l),88-101.
[56]. Wevu, N. (2006). Cosmic rays constituents of annual Radiation, *Australians Journal of Atmospheric Radiation,* 2(44),400-450.
[57]. Zhang, G., Burlaga, L.F. (1988). Magnetic clouds, geomagnetic disturbances, and cosmic ray decreases. *J. Geophys. Res.,* 93, 2511.